Fast atom diffraction inside a molecular beam epitaxy chamber, a rich combination

M. Debiossac[a], P. Atkinson[b], A. Zugarramurdi[a], M. Eddrief[b], F. Finocchi[b], V.H. Etgens[b],
A. Momeni[a], H. Khemliche[a], A.G. Borisov[a], P. Roncin[a,*]

[a] Institut des Sciences Moléculaires dOrsay (ISMO), CNRS, Univ. Paris-Sud, Université Paris-Saclay, Orsay F-91405, France
[b] Sorbonne Universités, UPMC Univ Paris 06, CNRS-UMR 7588, Institut des NanoSciences de Paris, F-75005 Paris, France

ARTICLE INFO

ABSTRACT

Two aspects of the contribution of grazing incidence fast atom diffraction (GIFAD) to molecular beam epitaxy (MBE) are reviewed here: the ability of GIFAD to provide *in-situ* a precise description of the atomic-scale surface topology, and its ability to follow larger-scale changes in surface roughness during layer-by-layer growth. Recent experimental and theoretical results obtained for the He atom beam incident along the highly corrugated $[1\bar{1}0]$ direction of the $\beta_2(2 \times 4)$ reconstructed GaAs(001) surface are summarized. We also discuss the measurements and calculations for the beam incidence along the weakly corrugated [010] direction where a periodicity twice smaller than expected is observed. The combination of the experiment, quantum scattering matrix calculations, and semiclassical analysis allows structural characteristics of the surface to be revealed. For the in situ measurements of GIFAD during molecular beam epitaxy of GaAs on GaAs surface we analyze the change in elastic and inelastic contributions in the scattered beam, and the variation of the diffraction pattern in polar angle scattering. This analysis outlines the robustness, the simplicity and the richness of the GIFAD as a technique to monitor the layer-by-layer epitaxial growth.

© 2016 Elsevier B.V. All rights reserved.

1. Introduction

Molecular beam epitaxy (MBE) has played a major role in the development of modern electronic devices. Its ability to deposit successive layers of high purity crystalline materials with monolayer accuracy is well established. Since its development, MBE growth has been monitored *in-situ* by reflection high energy electron diffraction [1] (RHEED). More recently, a new diffraction technique, grazing incidence fast atom diffraction (GIFAD) using the same geometry as RHEED but with keV atoms instead of electrons has emerged as a tool to measure the surface crystalline order on metals [2,3], semi-conductors [4,5] and insulators [6–8]. To test this technique under conventional semiconductor growth conditions, we have attached a GIFAD setup to a conventional III-V MBE chamber [9,4], and studied the surface reconstructions and dynamics of layer by layer growth for the homoepitaxy of GaAs.

The paper is organized as follows: firstly a discussion of the GIFAD technique and underlying theory is given, followed by details of its experimental implantation on a commercial MBE system. The measurement of the surface corrugation of a complex surface reconstruction: the $\beta_2(2 \times 4)$ reconstruction of the GaAs(001) surface is then discussed. Finally an analysis of the change in elastic and inelastic scattering, and the variation in polar angle intensity distribution of the scattered He atoms during layer-by-layer growth is presented.

2. Grazing incidence fast atom diffraction

Being unable to penetrate the topmost layer, thermal energy helium atoms are, by nature, perfectly surface sensitive. GIFAD uses helium atoms at energies E_0 in the range from some hundreds of eV to some keV impinging at the surface under grazing incidence angles $\theta \simeq 1°$. The full diffraction pattern can be then recorded with high efficiency on a position sensitive detector. The grazing incidence conditions correspond to very different regimes of the projectile motion parallel and perpendicular to the surface which typically can be treated separately. The motion parallel to the surface is fast leading merely to the averaging of the projectile-surface interaction potential along its trajectory. The diffraction is
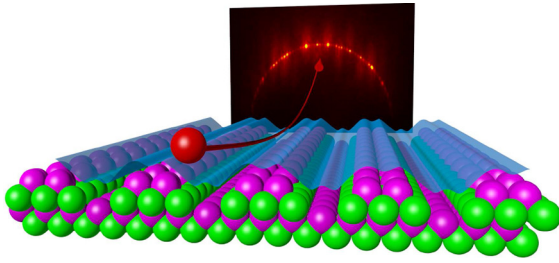
Fig. 1. An artist view of a fast helium atom diffracting on the rows of well aligned atoms of the $\beta_2(2 \times 4)$ GaAs surface along the [1$\bar{1}$0] direction. The hard corrugated wall model resulting from the projectile-surface potential averaged in the direction of the fast motion is displayed here as a blue sheet. It is often used to get simple intuitive insight into the GIFAD data. (For interpretation of the references to color in this figure legend, the reader is referred to the web version of the article.)

Fig. 2. Schematic view of the MBE chamber, with effusion cells evaporating gallium and arsenic onto a GaAs(001) wafer and the GIFAD setup replacing or complementing RHEED. A beam of He$^+$ ions is extracted at keV from a commercial ion source and then neutralized before entering the chamber. A variable aperture inside the chamber, approx. 10 cm from the sample surface ensures good collimation of the beam. The atoms scattered by the surface are imaged onto a position sensitive detector.

associated with slow motion perpendicular to the surface which corresponds to the projectile energy $E_\perp = E_0 \sin^2\theta$ in the sub-eV range. Indeed, the corresponding wavelength $\lambda_\perp = 2\pi/\sqrt{2ME_\perp}$ is in the Å range (M is the projectile mass). For further insights on the physics behind GIFAD we address the reader to Refs. [7,10–12].

One of the advantages of GIFAD over thermal energy helium atom scattering (HAS) [13–17] in that diffraction is preserved even at high substrate temperatures. In HAS the fraction of coherent scattering I_c/I_{tot} is described by the Debye Waller factor DW, $I_c/I_{tot} = e^{-DW}$ with $DW = -2(\delta k_\perp u_z)^2$ often forcing experiments to be performed on surface cooled at liquid nitrogen temperature. In GIFAD, the momentum transfer needed for specular reflection $2\delta k_\perp$ is spread over N successive atoms of the surface so that the effective thermal amplitude is $u_{eff} = u_z/\sqrt{N}$ and the effective Debye Waller factor is now N times smaller $DW_{eff} = DW/N$ giving rise to a much larger coherence ratio [18,10]. This explains that both larger perpendicular energies and higher surface temperatures can be studied in GIFAD. Another specificity of GIFAD is that only one Laue circle is typically observed [19] just as if the surface consists of translation-invariant furrows [7,20,22] (see Fig. 1). Finally, since the interaction reflecting the helium atom from the surface is comparable to that repelling the tip of an AFM, GIFAD can be interpreted in simple topological terms. In this respect it can be, metaphorically, seen as an AFM operating in the k-space.

3. Experimental setup MBE and GIFAD

The MBE chamber is a standard RIBER Compact21 but a splitting flange has been attached to both the source and detector RHEED ports allowing operation of RHEED or GIFAD independently [4,9]. The GIFAD setup is based on a conventional VG EX05 hot filament ion source. The He$^+$ ion beam extracted from the source enters a charge exchange cell filled with helium where 10–20% of the ions are neutralized by resonant electron capture. The ions that are not neutralized are deflected, and the resulting atom beam is collimated by two sets of diaphragms half a meter apart which also allow an efficient differential pumping. These diaphragms can limit the angular divergence of the beam down to the 0.01° range, but with a loss of beam intensity. The detector is made of one or two microchannel plate electron multipliers facing a phosphor screen which is imaged by a CCD camera. The GIFAD source was attached to the MBE chamber by flexible bellows, and could be "rocked" mechanically using automated motors to vary the incidence angle of the beam on the surface (Fig. 2).

Overall the use of GIFAD is comparable to that of RHEED, with a highly ordered 2D surface giving rise to bright spots centered on the Laue circle (Fig. 3). In GIFAD these spots inherit the profile of the incident beam. In addition, the inelastic background produced by the thermal movement of the surface atoms [10,18], and by the
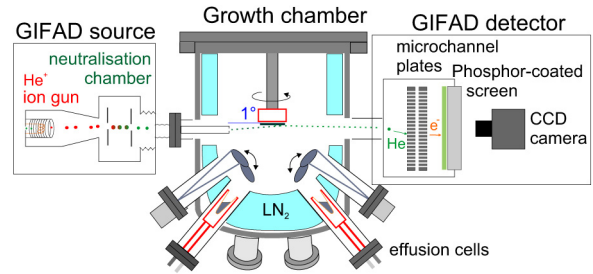
surface defects [23] gives rise to low intensity vertical extensions of the spots as can be seen in Fig. 1.

4. Static conditions, high resolution mode

4.1. The surface electronic density

When acquisition time is not an issue, the beam divergence can be reduced down to 0.01° resulting in a transverse momentum divergence $\delta k_\perp = k_0\delta\theta$, and a lateral coherence $2\pi/\delta k_\perp$ above 20 Å. The drawback is that the beam intensity is also reduced however extremely rich and complex diffraction patterns with up to almost one hundred diffraction spots can be recorded with good resolution in a still reasonable time of few minutes. The unit cell lattice spacing divided by the number of diffraction orders gives a rough measure of the lateral resolution of the surface potential corrugation while a vertical resolution of better than $\lambda_\perp/10$ is easily achieved due to the intrinsic interferometric accuracy. Under the collimation conditions discussed here, using 400 eV Helium atoms with incidence angle <1° yields a lateral resolution of 0.1 Å and a vertical resolution of 0.01 Å. Such an accuracy challenges the best theoretical descriptions of the surface, as was demonstrated in a combined theoretical and experimental GIFAD study of the $\beta_2(2 \times 4)$ reconstructed GaAs(001) surface [4]. In this work, the surface structure and projectile-surface interaction potential were obtained from *ab-initio* density functional theory (DFT) calculations. With the DFT inputs, the diffracted intensities were calculated using a close coupling technique and compared with experimental data. In the following we shortly review these results.

In Fig. 4 we show a small area of the experimental and theoretical diffraction charts corresponding to the $\beta_2(2\times4)$ reconstructed
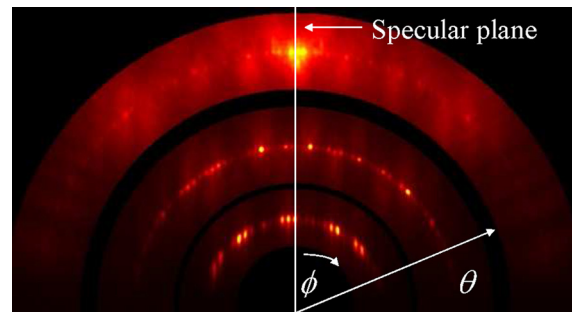

Fig. 3. Artificial assembly of three diffraction patterns recorded with 400 eV helium atoms incident along the [1$\bar{1}$0] direction of the $\beta_2(2\times4)$ reconstructed GaAs(001) surface at 530 °C. The radii of the different zero-order Laue circles is a direct measure of the polar angle of incidence θ corresponding to perpendicular energies $E_\perp$ of 17 meV, 55 meV, and 137 meV.